The variability in Gaseous Elemental Mercury at Villum Research Station, Station Nord in North Greenland from 1999 to 2017

[1]*Henrik Skov, [1]Jens Hjorth, [1]Claus Nordstrøm, [1]Bjarne Jensen, [1]Christel Christoffersen, [1]Maria Bech Poulsen, [1,2]Jesper Baldtzer Liisberg, [3]David Beddows, [4]Manuel Dall'Osto and [1]Jesper Christensen

5 *Corresponding author, [1]iClimate, Department of Environmental Science, Aarhus University, Frederiksborgvej 399, 4000 Roskilde, Denmark. [2]Physics of Ice, Climate and Earth, University of Copenhagen, Tagensvej 16, 2200 København N, Denmark. [3]Centre for Atmospheric Science Division of Environmental Health & Risk Management School of Geography, Earth & Environmental Sciences, University of Birmingham, Edgbaston Birmingham, B15 2TT, United Kingdom. [4]Institute of Marine Sciences (ICM) Consejo Superior de Investigaciones Científicas (CSIC), Pg. Marítim de la Barceloneta 37–49, 10 08003, Barcelona, Spain.

Correspondence to: Henrik Skov (HSK@ENVS.AU.DK)

Abstract. Mercury is ubiquitous in the atmosphere and atmospheric transport is an important source for this element in the Arctic. Measurements of gaseous elemental mercury (GEM) have been carried out at the Villum Research Station (Villum) at Station Nord, situated in north Greenland. The measurements cover the period 1999-2017 with a gap in the data for the period 15 2003-2008 (for a total of 11 years). The measurements were compared with model results from the Danish Eulerian Hemispheric Model (DEHM) model that describes the contribution from direct anthropogenic transport, marine emission and general background concentration. The percentage of time spent over different surfaces was calculated by back-trajectory analysis and the reaction kinetics was determined by comparison with ozone.

The GEM measurements were analysed for trends, both seasonal and annually. The only significant trend found was a negative 20 one for the winter months. Comparison of the measurements to simulations using the Danish Eulerian Hemispheric Model (DEHM) indicated that direct transport of anthropogenic emissions of mercury accounts for between 14 and 17% of the measured mercury. Analysis of the kinetics of the observed Atmospheric Mercury Depletion Events (AMDEs) confirms the results of a previous study at Villum of the competing reactions of GEM and ozone with Br, which suggests a lifetime of GEM on the order of a month. However, a GEM lifetime of 12 months gave the best agreement between model and measurements. 25 The chemical lifetime is shorter and thus the apparent lifetime appears to be the result of deposition followed by reduction and reemission; for this reason the term 'relaxation time' is preferred to 'lifetime' for GEM. The relaxation time for GEM causes a delay between emission reductions and the effect on actual concentrations.

No annual trend was found for the measured concentrations of GEM over the measurement period despite emission reductions. This is interesting and together with low direct transport of GEM to Villum, as found by the DEHM model, it shows that the 30 dynamics of GEM is very complex. Therefore in the coming years, intensive measurement networks is highly needed to describe the global distribution of mercury in the environment as the use of models to predict future levels will still be highly uncertain. The situation is increasingly complex due to global change that most likely will change the transport patterns of mercury not only in the atmosphere but also between matrixes.

1 Introduction

35 The effects of long-range atmospheric transport of anthropogenic pollutants into the Arctic are well documented: contaminants are affecting the Arctic by contamination of food chains, and by altering the radiation budget, and by that contributing to climate change (UNEP 2013; AMAP/UNEP 2013, Heidam et al. 2004). Until now, there are only few local sources of pollutants in the Arctic and long-range transport mainly from mid latitudes represent the main source.

Mercury (Hg) is one of the first substances that have been identified as a pollutant in the food web worldwide, causing adverse

40 effects to human health and wildlife. On this background the Minamata Convention, aiming at reducing the exposure of human beings and the environment to mercury, was established in 2013; the convention entered into force in 2017.

The sources of mercury in the environment can be divided into natural, anthropogenic, and reemission, accounting for roughly 10, 30 and 60% of the emissions, respectively. The global anthropogenic emissions of mercury were estimated as 1960 tonnes in 2010, however with large uncertainties (UNEP 2013; AMAP/UNEP 2013). According to an estimate by (Pirrone et al. 2010)

45 natural sources and reemission processes (hereafter referred to as ´background sources´), accounted for 5207 Mg per year in 2005 while the amount of new anthropogenic inputs is 2320 Mg per year. According to recent assessments (Pacyna et al. 2010; Pirrone et al. 2010; AMAP/UNEP 2013; UNEP 2013; Muntean et al. 2014), main anthropogenic sources of atmospheric mercury are coal combustion and artisanal/small gold mining, with relevant contributions from non-ferrous metal/steel combustion along with several other industrial/residential sources such as waste incineration. The main background source is

50 evasion from ocean surfaces, accounting for about half of the sum of the natural and reemission contributions (Pirrone et al. 2010). Reemission of deposited atmospheric mercury of anthropogenic origin gives a major contribution to the reemission budget, e.g. it has been found that the accumulation of mercury inputs from anthropogenic sources to oceans have led to an increase of mercury in surface waters of about a factor of three (Lamborg et al. 2014)). Mercury is transported by rivers, sea currents, and in the troposphere. Mercury in air is mainly found in the gas phase, where the major part is gaseous elemental

55 mercury (GEM) covering more than 90%, while a minor part is oxidized mercury as well as in particles. The share of oxidized mercury of the overall global emissions of mercury has been estimated to be around 25%, based on speciation factors from the Arctic Monitoring and Assessment Program (Muntean et al. 2018). The atmospheric lifetime of GEM has been estimated to be in the range of about one year while those of oxidized forms of mercury are shorter (Steffen et al. 2008). The lifetime is however under dispute and evidence has been obtained from experimental and theoretical studies for a much shorter lifetime

60 of GEM (Skov et al. 2004; Goodsite, Plane, and Skov 2004; Holmes et al. 2010; Soerensen et al. 2010; Goodsite, Plane, and Skov 2012a). The deposition rate depends on the chemical processes that transform GEM into the less volatile Hg^{II} species; these processes are only partially understood (Angot et al. 2016). Chemical conversion of GEM to Hg^{II} seems to be particularly important in the Arctic area where ozone and mercury chemistry have been found to be coupled during events where both are observed at ground level to be depleted from the air. There is strong evidence that these depletion episodes are caused by the

65 photochemical formation of bromine atoms (Skov et al. 2004; Goodsite, Plane, and Skov 2004, 2012a; Skov et al. 2006; Kamp et al. 2018) and recently direct evidence was found for Br initiated AMDEs and ODEs (Wang et al. 2019).

The geographical distribution of the emissions have changed in the last decades, where Asian countries have gained importance compared to emissions in Europe, North America, and Japan. Today China accounts for about 40% of the global Hg emission (Muntean et al. 2014; Jiskra et al. 2018). In North America, Europe and on the North Atlantic Ocean there is seen a decline in the GEM concentration of between -1.5 and 2.2% yr^{-1} (Obrist et al. 2018). In the Arctic the decline is zero at Svalbard (Berg et al. 2013) and -0.9% at Alert (Cole et al. 2013).

The aim of the present article is to present and discuss the long time series of GEM measurements at Villum Research Station at Station Nord in North Greenland with a focus on observed inter-annual and seasonal trends as well as the likely explanations for these in terms of sources, transport patterns and dynamics.

2 Experimental section

2.1 Measurements

Villum Research Station (Villum) at Station Nord in North Greenland is the second most northerly, permanently open station in the Arctic only preceded by Alert, Canada. The station has all the logistic requirements and infrastructures that are necessary for being a major international platform for scientific studies focused on the Arctic cryosphere, nature and interaction with humans. It is located in the farthest north-eastern corner of Greenland on the north-south oriented peninsula Princesse Ingeborgs Halvø (a small Peninsula, 81°36' N 16°40' W) which northern end is a 20 x 15 km^2 Arctic lowland plain (see Figure 1). Villum is an important logistic site for many scientific research activities in the Greenlandic National Park, in North Greenland, see www.villumresearchstation.dk. Ozone and GEM were measured at Flygers Hut from 1996 and 1999, respectively, to 2015 when the measurements were moved to the newly built Air Observatory (Figure 2) and continue to this day.

Since 1999, GEM has been measured by a TEKRAN 2537 mercury analyser. In the first years, funding was only available for six month per year of observations and thus the data coverage over the entire year is limited to spring, summer and early autumn except for the very first year. There are no measurements available for the years 2003-2008 as the research station was closed. Several generations of the instrument have been used (A, B and X versions) but we estimate that the uncertainty of measuring GEM has remained unchanged during the years. The principle of the instrument is as follows: a measured volume of sample air is drawn through a gold trap that quantitatively retains elemental mercury. The collected mercury is desorbed thermally from the gold trap and is transferred by argon into the detection chamber, where the amount of mercury is detected by cold vapour atomic fluorescence spectroscopy. The detection limit is 0.1 ng m^{-3} and the reproducibility for concentrations above 0.5 ng m^{-3} is within 20 % based on parallel measurements with two TEKRAN 2537A mercury analysers (at a 95 % confidence interval). The calibration of the instrument is checked every 25 hours by adding known quantities of elemental mercury to the detection system from an internal permeation source. The sample air was either taken through a sample tube heated to 50° C or by drawing sample air from a 20 cm i.d. stainless sample tube. The flow rate in the stainless tube was > 1

m³ min⁻¹. Comparison of measurements from the two different sample lines did not reveal any difference within the uncertainty of the instruments. Prior to entering the instrument air passes a soda lime trap to avoid passivation of the gold traps.

100 Ozone has been measured since 1996. Though different instruments have been applied, the measurement uncertainty is unchanged as the basic principle in all instruments is absorption of UV light at 254 nm. The stability of the instruments is ensured by addition of known concentrations of ozone from an internal ozone generator traceable to a primary standard. The uncertainty at a 95 % confidence level is <7% for concentrations above 20 ppbv and 1.4 ppbv for concentrations below 20 ppbv.

105 We have applied the Danish Eulerian Hemispheric Model (DEHM) to calculate the concentrations and direct contributions from different source areas to the concentrations levels at Villum as a function of a prescribed chemical lifetime of Hg^0 and the meteorological variability of the atmospheric transport from source areas.

2.2 Model calculations

DEHM is a three-dimensional, offline, large-scale, Eulerian, atmospheric chemistry transport model (CTM) developed to study
110 long-range transport of air pollution in the Northern Hemisphere with focus on Arctic or Europe. The model domain used in previous studies covers most of the Northern Hemisphere, discretized on a polar stereographic projection, and includes a two-way nesting procedure with several nests with higher resolution over Europe, Northern Europe and Denmark or Arctic (Frohn, Christensen, and Brandt 2002; Brandt et al. 2012).

DEHM was originally developed in the early 1990's to study the atmospheric transport of sulphur and sulphate into the Arctic
115 (Christensen 1997; Heidam, Wåhlin, and Christensen 1999; Heidam et al. 2004) and has also been used to study transport of Mercury to the Arctic (Christensen et al. 2004, Skov et al. 2004).

The model system has been setup with one model domain with 150x150 grid points. The domain covers the northern hemisphere with a grid resolution on 150 km at 60°N. The vertical grid is defined using the σ-coordinate system, with 29 vertical layers extending up to a height of 100 hPa.

120 The DEHM model is driven by meteorological data from the Advanced Research WRF version 3.6 (WRF ARW) (Skamarock et al., 2008). This WRF model simulation was driven by global meteorological ERA-Interim data, which is a global atmospheric reanalysis data set from the European Centre for Medium-Range Weather Forecasts (ECMWF) starting from 1979 and continuously updated in real time. These data have been nudged every 6 hour into the WRF model. The WRF model has been run in a climate mode setup, e.g. continuously updating Sea Surface Temperature and deep soil temperature (both from
125 the ERA interim).

The global historical AMAP Hg emissions inventories 1999 to 2017 have been used for the anthropogenic emissions (UNEP 2013). Emissions of mercury from biomass burning was based on CO emissions obtained from Global Fire Emissions Database, Version 3, (van der Werf et al. 2006; Van der Werf et al., 2003) where a fixed Hg^0/CO ratio of 8×10^{-7} kg Hg/kg CO. Emissions from oceans are based on calculated fluxes from the GEOS-Chem model (Soerensen et al. 2010). The anthropogenic
130 emissions are variable up to 2010 where after they are constant.

The system has been set up with 11 different tracers, which represent 8 different anthropogenic source areas (Russia, Eastern Europe, Western Europe, China, North America, Rest of Asia, Africa and South America), biomass burning, ocean sources and the prescribed boundary conditions on 1.5 ng/m^3 for the entire period. The latter is introduced because of the long lifetime of Hg^0 and accounts for the transport across equator with the exchange velocity between the two hemispheres of about 1 year.

135 The boundary condition is also introduced to account for all emissions in both hemispheres. There have been made three different model runs covering the period from 1990 to 2017, where each model run has a fixed first order reaction lifetime for Hg^0 of 1 month, 6 months and 1 year, respectively. The boundary conditions were kept constant during the period covered by the model. The model does not include Arctic mercury depletion in the runs presented here; it focuses only on the direct long-range transported mercury contribution to the GEM concentration at Villum.

2.3 Trajectory model

140

In order to investigate the influence of different surfaces on GEM concentration, 120 hours back trajectories for air masses arriving at 100 m altitude at Villum were calculated with hourly resolution using the BADC (British Atmospheric Data Centre) Trajectory Service. For each of the trajectories the time spent over different surfaces was calculated using a polar stereographic map of the Northern Hemisphere, where each of the 1024x1024 24 km grid cells were classified as land, sea, snow or sea ice,

145 and thus the percentage of the total transport time spent over these four types of surfaces could be calculated. The snow and ice coverage values were generated by the NOAA/NESDIS Interactive Multisensor Snow and Ice Mapping System (IMS) developed by the Interactive Processing Branch of the Satellite Services Division. For what concerns the sea ice coverage, a similar calculation was performed using daily stereographic maps of sea ice concentration with a resolution of 12.5 km, available also from NOAA/NESDIS. This calculation allowed to establish the percentage of time where the air mass of the

150 back trajectory was passing over sea ice as done earlier in studies of atmospheric particle dynamics (Dall'Osto et al. 2018). Combining these calculations for the periods where GEM measurements were carried out at Villum, the percentages of the 120 hour duration of the trajectory, where the air masses passed over land, sea, snow and sea ice surfaces could be established.

3 Results and discussion

The measurements of GEM and ozone from 1996 to 2017 are shown in Figure 3. A seasonal pattern is observed for each year.

155 In January and February, the level of ozone and GEM is rather stable. After the polar sunrise, the concentration starts to fluctuate strongly and ozone and GEM are depleted fast (during 2 to 10 hours). Figure 4 shows the variations of the yearly average GEM concentration and the average for the winter season between 1999 and 2017, where only periods with more than 50% data coverage have been included. The yearly and seasonal averages and their trends as well as their uncertainty limits (assuming a normal distribution of the measurement data around the regression line) are shown in Table 1. The annual averages

160 do not show any significant trend at 95% confidence interval (Table 1). This lack of yearly trend is the result of a combination of rather different seasonal trends: in the autumn (September-October-November) there is an insignificant decrease (-

0.87%/yr), whereas in winter (December-January-February) a pronounced decrease of -1.56%/yr is observed (significant on 95% confident interval). A test of the importance of the value in 2000 showed that the decrease is almost unchanged removing the point but R^2 falls to 0.29 though the trend is still significant. In the spring (March-April-May) there is not any significant

165   trend, though a small positive trend is seen (0.35%/yr). For the summer (June-July-August) there is a positive trend of 0.75%/yr that however is not significant. This result is similar to the result obtained at Zeppelin Station on Svalbard for the period 2000 to 2008 (Berg et al. 2013) and, as previously mentioned, at Alert, Canada, where a negative trend of -0.009 ng/m^3 (-0.58%/yr) is seen for the period between 1995 and 2008 (Steffen et al. 2015). In a study of GEM in firn snow from the Greenlandic inland ice at about 3 km altitude, Dommercue et al. (2016) showed that there is a positive trend or no trend during the period 2000-

170   2010, though the authors pointed out that nothing conclusively can be said about the concentration trends based on their results. The behaviour of the trends may in principle be explained by changes in the emissions in the source regions, in transport patterns, in deposition, re-emission as well as atmospheric chemistry. The seasonal differences in the trends must be explained by a different influence of these factors during the different seasons. Finally, it has been suggested that decreasing GEM concentrations in the Northern Hemisphere over the last 20 years may be partially explained by increased uptake by vegetation

175   due to increased net primary productivity (Jiskra, 2018). In the following section, we will discuss these possible explanations for the observed trends separately.

3.1 Changes in atmospheric chemistry

The strongest concentration trend is found during the winter, where photochemically driven chemistry obviously does not take place in the area but where long range transport from mid-latitudes is at its maximum. The main influence of Arctic atmospheric

180   chemistry on GEM concentrations is expected to be in the spring and summer period, where the fate of GEM is believed to depend on the presence of seasonal sea ice and the presence of air temperatures below -4°C (Christensen et al. 2004). Figure 5 shows a conceptual description of mercury removal in Arctic. Also a regression analysis of the number of hours with depletion events (defined here as GEM< 0.5 ng/m3) did not show any significant change over the years 2000-2017. Neither the ozone data obtained during the period 1999-2017 did show any significant trend for the concentrations in spring or summer.

185   The ozone observations will be the subject of a separate publication.

The data until 2002 were used to investigate reaction kinetics of ozone and GEM with a third reactant. Log – log plots of ozone against GEM gave a straight line as seen earlier (Schroeder et al. 1998; Berg et al. 2003; Steffen et al. 2008; Skov et al. 2004). A reaction rate for Br with Hg^0 was calculated, which fitted well with a reaction rate determined by theoretical chemistry (Goodsite, Plane, and Skov 2012b; Goodsite, Plane, and Skov 2004; Skov et al. 2004). We made the same analysis on the data

190   from 2007 and onwards. GEM was averaged to a time resolution of 0.5 hour. The new analysis confirmed the previous result, though the data points were more scattered and thus the resulting slope was connected with a larger uncertainty, mostly due to smaller difference between the initial GEM concentration and the final concentration. An important point for the parameterisation of GEM depletion is that atmospheric mercury depletion event (AMDE often was observed under stagnant wind conditions

195   As shown in Table 1, the seasonal averaged concentration has a maximum in the summer (June-July-August) and a minimum in the spring (March-April-May). In order to test the hypothesis that the spring minimum is related to the occurrence of the combined mercury and ozone depletion events, an indicator of the duration and frequency of such depletion episodes was created. The number of measured hourly GEM concentrations below 50% of the average value in a previous event free period was compared, as a percentage, to the total number of available hourly measurements during the period of interest. For the

200   March-April-May period this percentage of AMDE hours was found to be strongly correlated with the average GEM concentrations in the same period (Figure 6). Thus, there is evidence for a strong impact of AMDE on GEM concentrations in the spring period. Frequency of AMDE and GEM concentration in summer showed a poor negative correlation. If the deposited Hg during AMDE should be released again during snowmelt, a positive correlation would have been expected, but this was not observed. In fact, the analyses indicate that AMDE is a net sink for mercury, which is in agreement with direct flux

205   measurements (Brooks et al. 2006). Even the annual mean value had a negative correlation with AMDE hours. Though this correlation is weak, it is an indication that AMDEs affect the GEM concentration level at Villum.

It has been determined that outflows from rivers are a main source of Hg in the Arctic Ocean (e.g. Outridge et al. 2008, Fischer et al. 2012). The present study indicates that atmospheric input can be significant as well. A very important step in the determination of the significance of these sources for understanding Hg accumulation in the food web is to determine the

210   bioavailability of mercury deposited (Moller et al. 2011) compared to that from river discharge.

3.2 Decrease in the emissions in the source regions

Recent studies show that mercury emissions from Europe and North America have been decreasing since 1990, while emissions in Asia have been increasing (UNEP 2013; Muntean et al. 2014). Russian emissions, considered as a separate entity, have been decreasing as well. Concentration data from cruises on the North Atlantic show a declining trend since 1990 with a

215   steep decrease in the surface seawater Hg^0 concentration between the years 1998-2000 and 2008-2010 of -5.7% per year. It has been found that the corresponding decrease in mercury emissions from the sea can explain the decreasing trend observed over the North Atlantic and adjacent areas (Soerensen et al. 2012). Chen and co-workers (Chen et al. 2015) found that the decline in atmospheric concentrations at north-mid latitudes was significant for the period 2000-2009 but much weaker in the Arctic. They explained this by the fact that declining sea ice cover and increasing temperatures caused a tendency towards

220   higher emissions from the sea that (partially) compensates for the forcing by decreasing surface water Hg^0 concentrations in the North Atlantic. The observed seasonality with a much more significant declining tendency in the atmospheric GEM concentration in winter (DJF) than in spring (MAM) or summer (JJA) may be explained as suggested by Chen et al. The highest concentration of GEM was found in 2013, thereafter there has been a continuous decrease and that might be the effect of emission reductions that now is evident also in high Arctic.

225   The DEHM model, using variable anthropogenic emissions as described above, shows a slightly decreasing concentration trend, -0.7% per year (see Figure 7). However, this direct anthropogenic input, assuming an atmospheric lifetime of GEM of 12 months, does only account for between 14 and 17% of the observed GEM concentrations, (Figure 8). Including the impact

of sea emissions and of the boundary conditions, and assuming a GEM atmospheric lifetime of 12 months, the model predicts an annual average GEM concentrations of 1.40-1.43 ng/m^3, i.e. in agreement with the measured average in the period of 1.46

230   ng/m^3 , although the measured data covers a larger range of values (1.2 - 1.8 ng/m^3). When applying longer or shorter GEM lifetimes, the model results deviate more from the measured concentrations. This indicates that the best relaxation time of GEM in the Northern Hemisphere is 12 months. The chemical lifetime of GEM in the atmosphere is most likely shorter according to the theoretical and experimental evidence (e.g. Goodsite et al. 2004, 2012; Ariya et al. 2008, Donohoue et al. 2005, 2006; Dibble et al. 2012. Therefore, the deposition of Hg^{II} species appears to be followed by reduction and reemission

235   of Hg^0 (e.g. Brooks et al. 2006, Kamp et al. 2018, Soerensen et al. 2012, Steen et al. 2009, Cobbett et al. 2007). Thus, relaxation time seems to be a more appropriate name than lifetime for GEM. This is supported by a study on the photo-reduction of Hg^{II} in cloud droplets, which was found to be much slower than the one used in models leading to the conclusion that deposition and reemission are involved in the dynamics of atmospheric mercury (Saiz-Lopez et al. 2018). The sea emissions were found to account for 20-21% of the GEM concentration at Villum, and the boundary conditions on 1.5 ng/m^3 explained 62-65%,

240   while emissions from fires contributed by 1% during the years of the measurements, still assuming a 12 months GEM atmospheric lifetime.

In separate calculations with DEHM, it was found that emissions from China had larger relative importance during the summer than in the winter season; however, this difference was only significant for relatively short (less than 1 year) atmospheric lifetimes of GEM. Durnford et al. (2010), applying the GRAHM model, investigated the contribution of different source

245   regions to total mercury as well as GEM concentrations at several Arctic monitoring stations at different seasons of the year. They found that for the yearly concentration averages and their variability at the Arctic stations, including Villum, Asian emissions were the most important, accounting for more than the sum of the contributions from Europe, Russia and North America. The calculations for Villum were performed for the year 2001. This result is in agreement with the present study but in contrast to several studies addressing the origin of shorter-lived pollutants such as black carbon and sulphate that point to

250   the northerly part of Eurasia as the main source regions (Nguyen et al. 2016, Freud et al. 2017). Particularly in the case of Station Nord (now named Villum Research Station), Nguyen et al. 2013 found evidence of a strong influence of direct transport of particles from Siberia including results from previous work (Heidam et al. 2004). Heidam et al. identified Russia as the main contribution to sulphate concentrations, followed by East and Western Europe, while Asian contributions appeared to be of minor importance. The explanation for this difference between modelling results regarding mercury and more short-lived

255   air pollutants is likely to be the large difference in atmospheric lifetimes (relaxation time for GEM). The above discussion highlights the importance of assessing the chemistry of GEM and determining the fate of the resulting reaction products, especially the photo-reduction of Hg^{II} compounds in marine waters.

3.3 Changing transport patterns

Results obtained by applying the DEHM model to simulate GEM concentrations at Villum Research Station indicate that

260   changes in atmospheric transport cannot explain the observed trend. We have found that the simulated yearly and seasonal

GEM values show very little variability and no significant trend over the years 2000-2015, when the emission sources are kept constant at the 2005 level while the meteorology is varying and treated as described above. The study by Hirdman et al. (2010) of long term trends of sulphate and BC in the Arctic also concludes that changes in atmospheric transport can only explain a small fraction (0.3-7.2%) of the observed trends.

265 In an earlier paper on particle formation in Arctic atmosphere, important results have been obtained correlating the time airmasses spent over different surfaces (Dall'Osto et al. 2018). We did the same calculations for GEM data. The correlations between the time that air masses passed over different surfaces and the measured GEM concentrations at Villum are shown in Table 2. Relatively strong negative correlations ($R^2 > 0.3$) were found only in the autumn. Performing a two-tailed t-test it was found that the only significant correlation at a 90% confidence was the anticorrelation in the autumn with land ($R^2 = 0.44$)

270 while the anticorrelation with sea was significant only at an 85% confidence level ($R^2 = 0.32$). Different types of surfaces may influence deposition and emission rates for mercury, and they may have an influence on atmospheric chemistry, e.g. by release of reactive bromine compound. However, the correlations may also not be due to a relationship caused by the impact of the surfaces within the 120 hours' time span of the trajectories but rather by the longer term histories of the air masses. As the percentage of time passed over land by the air masses in the autumn months (SON) is very short (1-4% of the 120 hours) it

275 seems most likely that the correlation observed is not due to a direct influence of land. It can thus be concluded from the results shown in Table 2 that no statistically significant impact of surfaces on GEM concentrations within the range of the 120 hours back trajectories could be observed.

The DEHM model predicts that there is a maximum in GEM concentration during late winter and spring (data not shown) due to long-range transport. Such a behaviour is not observed in the measurements (Figure 3). In fact, the highest concentration of

280 GEM is observed during summer and is attributed to release of GEM from the melting snow and ice pack from mercury deposited during AMDEs in spring. However, emission from open sea may also be a plausible explanation (Chen et al. 2015).

4 Conclusion

In this paper, we present GEM concentrations from 1999 to 2017 with a break in the dataset from July 2002 until 2007. The large fraction of GEM assigned to background contribution and from sea makes it difficult to assess a trend from the otherwise

285 predicted emission reduction in the immediate source areas for mercury. A decreasing trend in the concentration of GEM was found during autumn and winter but was counteracted by a weak increase during the rest of the year. Therefore, there was not any significant trend in the yearly average concentrations at the 95% confidence level.

Simulations of the concentrations at Villum using the DEHM model using fixed emission inventory show no significant trends and thus it is concluded that the observed trends are not caused by changes in atmospheric transport patterns. The measurement

290 area is known to be strongly influenced by long-range transport of pollutants in the winter and spring period and the only viable explanation of the observed trend in the winter appears to be decreasing emissions in the source regions. However, according to the DEHM simulations the direct anthropogenic transport only accounted for between 14 and 17% of the GEM

concentration and might be counteracted by the hemispheric background on 1.5 ng/m^3 that accounts for 62-65% and was kept constant in the model. The boundary conditions represent contributions from indirect transport from sources on the Northern

295   hemisphere and transport from sources on the southern hemisphere. Similar considerations could be made about sea emission, accounting for 20-21%.

The seasonal variation confirms the effect of AMDE leading to generally lower concentrations during spring; in fact, a strong anticorrelation between the average GEM concentrations during springtime and the number of hours with AMDE conditions was observed. The analyses indicated that AMDEs are a net sink for mercury in the atmosphere and that it affects the yearly

300   average concentration.

Simulations with the DEHM model showed best agreement with observations applying an atmospheric lifetime of GEM of 12 months; however, it was found that the apparent lifetime is likely to be the result of a shorter chemical lifetime with respect to oxidation, followed by deposition, reduction and reemission. Thus, 'atmospheric relaxation time' seems to be a more appropriate term than 'lifetime' for GEM.

305   The lack of a trend in the measured concentrations of GEM despite emission reductions is striking but, together with low direct transport of GEM to Villum as found by the DEHM model, it shows that the dynamics of GEM is very complex. Therefore, in the coming years intensive measurement networks is strongly needed to describe the global distribution of mercury in the environment because the use of models to predict future levels will still be highly uncertain. The situation is increasingly complex due to global change that most likely will change the transport patterns of mercury not only in the atmosphere but

310   also between matrixes.

Table

Table 1. Mean values and yearly trends of the seasonal averages of the GEM measurements at Villum. The upper and lower limits are calculated for a 95% confidence limit. The data points and the trend lines are shown in Figure 4.

	DJF	MAM	JJA	SON	All
Mean value (ng/m^3)	1.48	1.29	1.63	1.42	1.46
Trend (% per year)	-1.56	0.35	0.75	-0.87	-0.42
Lower Limit (% per year)	-2.73	-2.45	-1.33	-2.28	-1,94
Upper limit (% per year)	-0.38	3.14	2.83	0.54	1,10

315
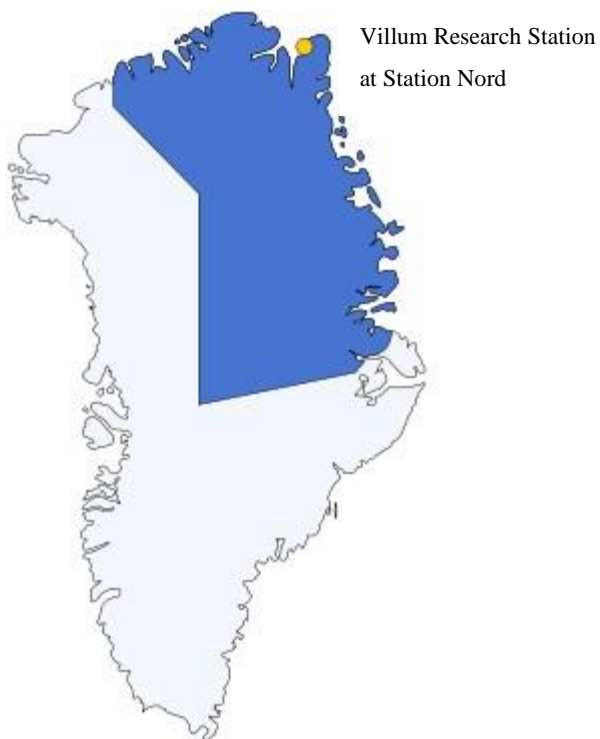
Figure 1: The position of Villum Research Station at Station Nord in North Greenland. The blue area represents the Greenlandic National Park.
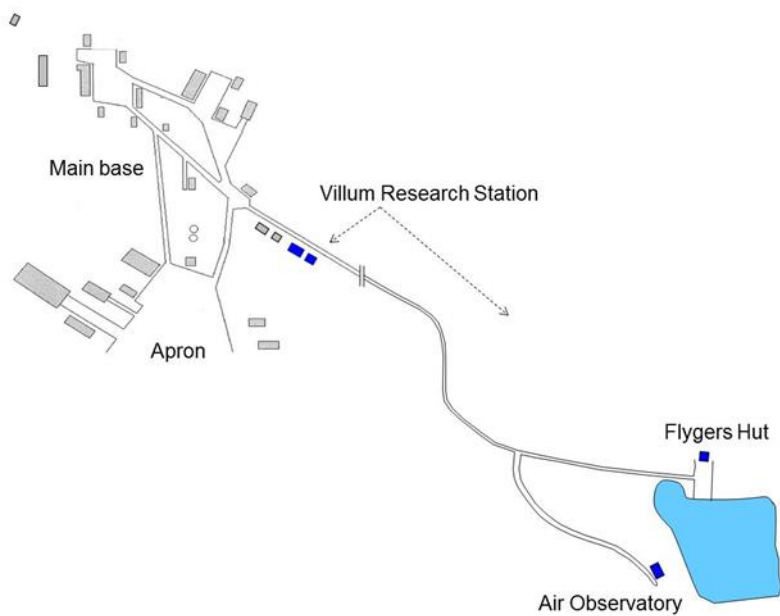
Figure 2: Map of Villum Research Station with its buildings (blue) relative to Station Nord military outpost. Flygers Hut and Air Observatory are located about 2 km outside main base of Station Nord. Until 2014 all measurements were performed in Flygers Hut, thereafter they were moved to Air Observatory.
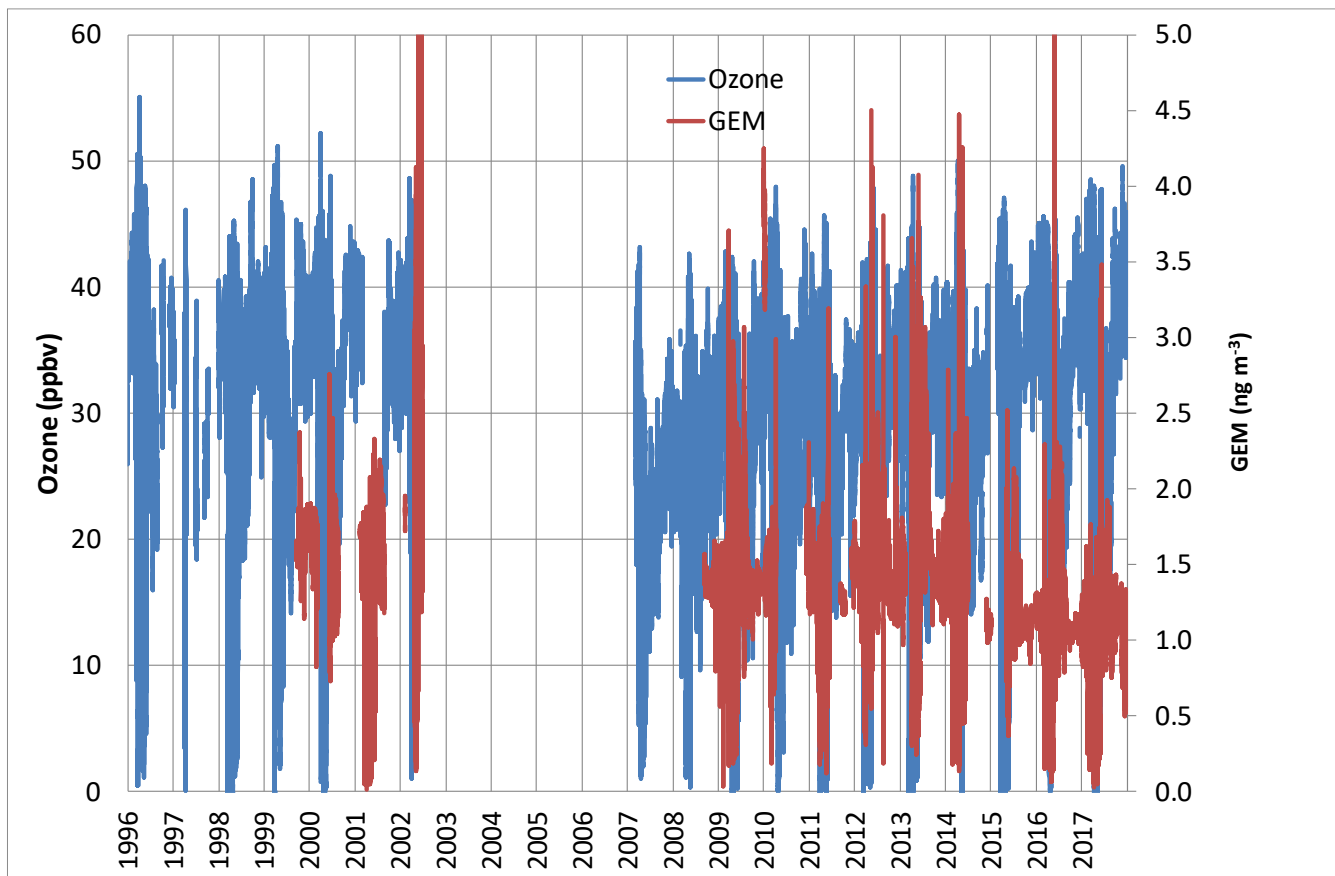
330

Figure 3: Time series of the concentration of GEM and the mixing ratio of ozone at Villum Research Station
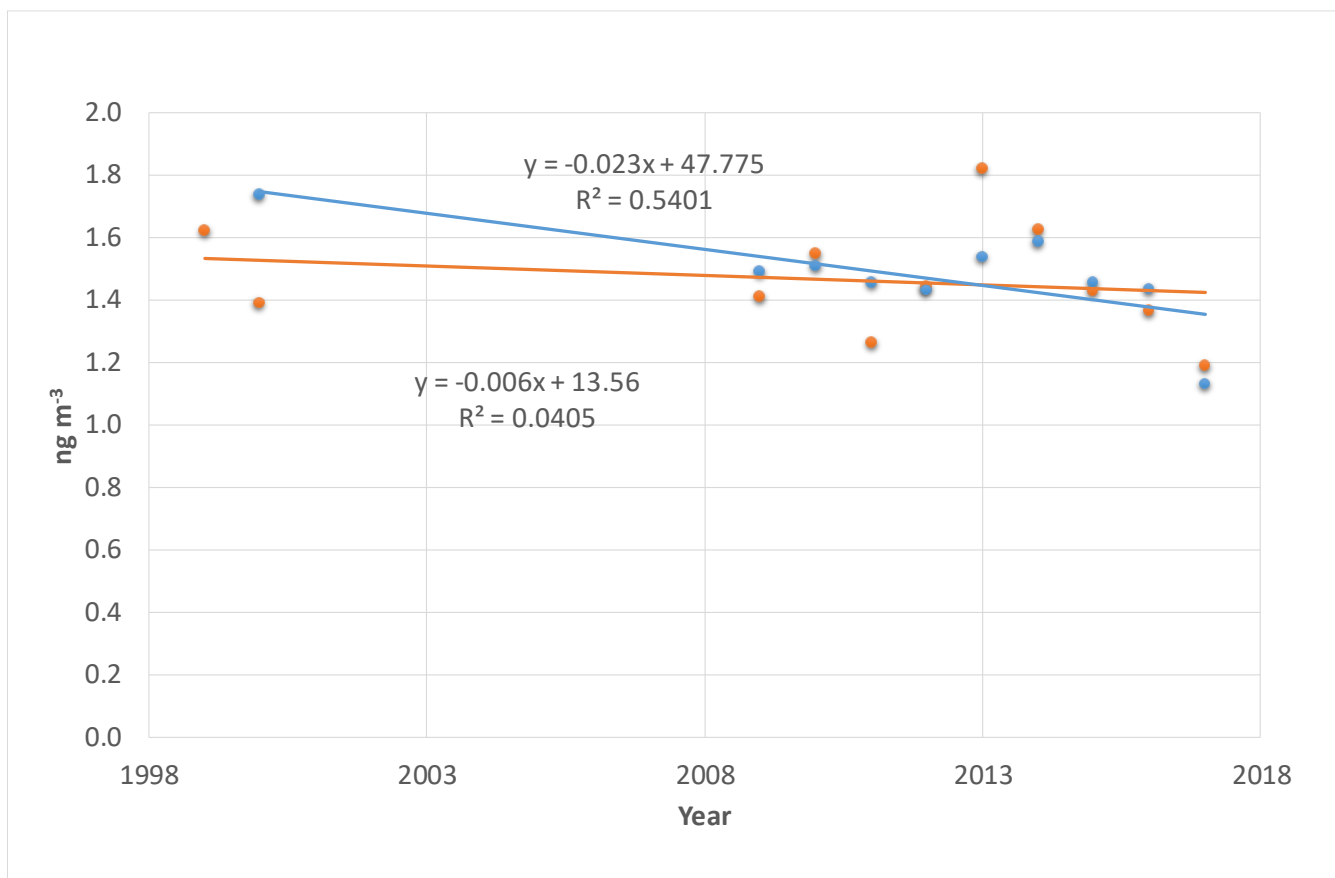
Figure 4: Yearly (Orange) and winter season (December-January-February, Blue) average values of measured GEM concentrations at Villum with trend lines.
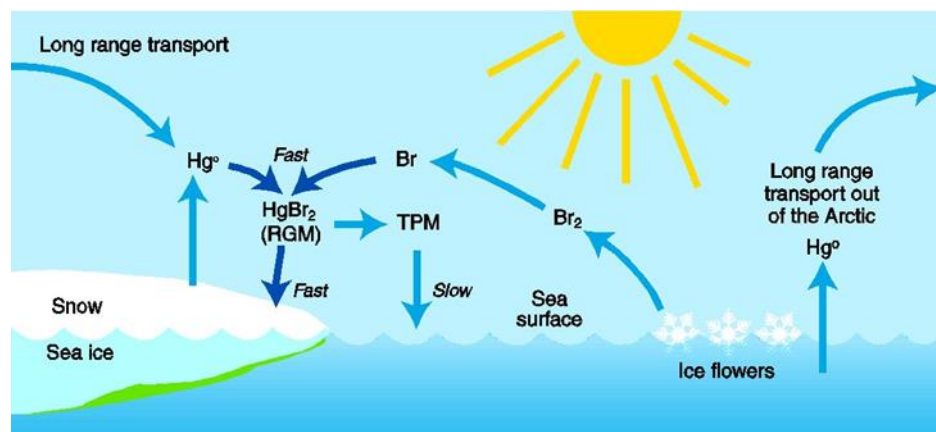
Figure 5: The mercury cycle in the Arctic atmosphere where gaseous elemental mercury (Hg⁰) is converted to reactive gaseous mercury (RGM) that is fast either deposited or converted into total particulate mercury (TPM). The chemical composition of RGM is unknown and HgBr₂ is one suggestion among many (From Henrik Skov in AMAP report 2013).
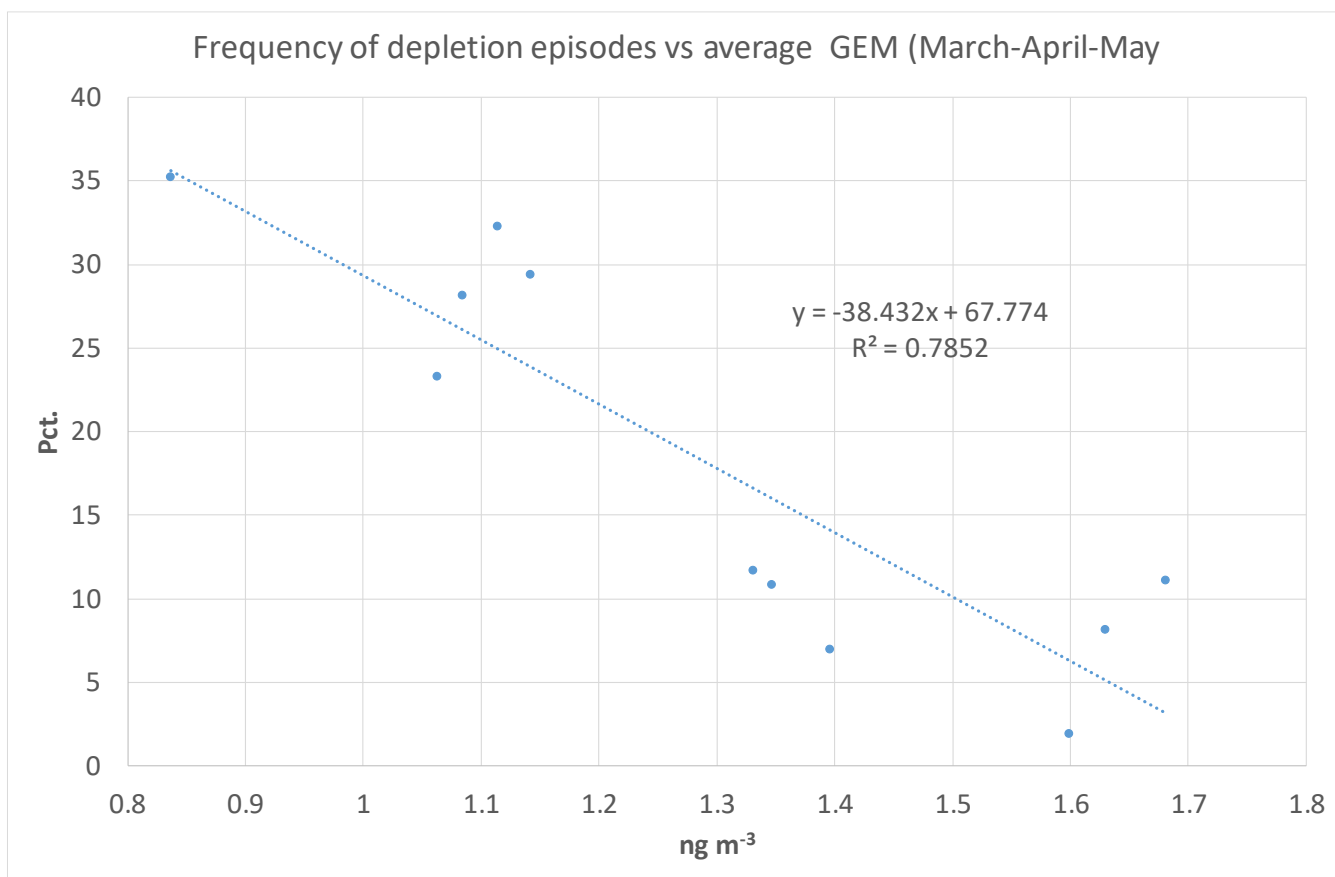
345

Figure 6: Frequency of depletion episodes versus average GEM concentration in March, April and May.
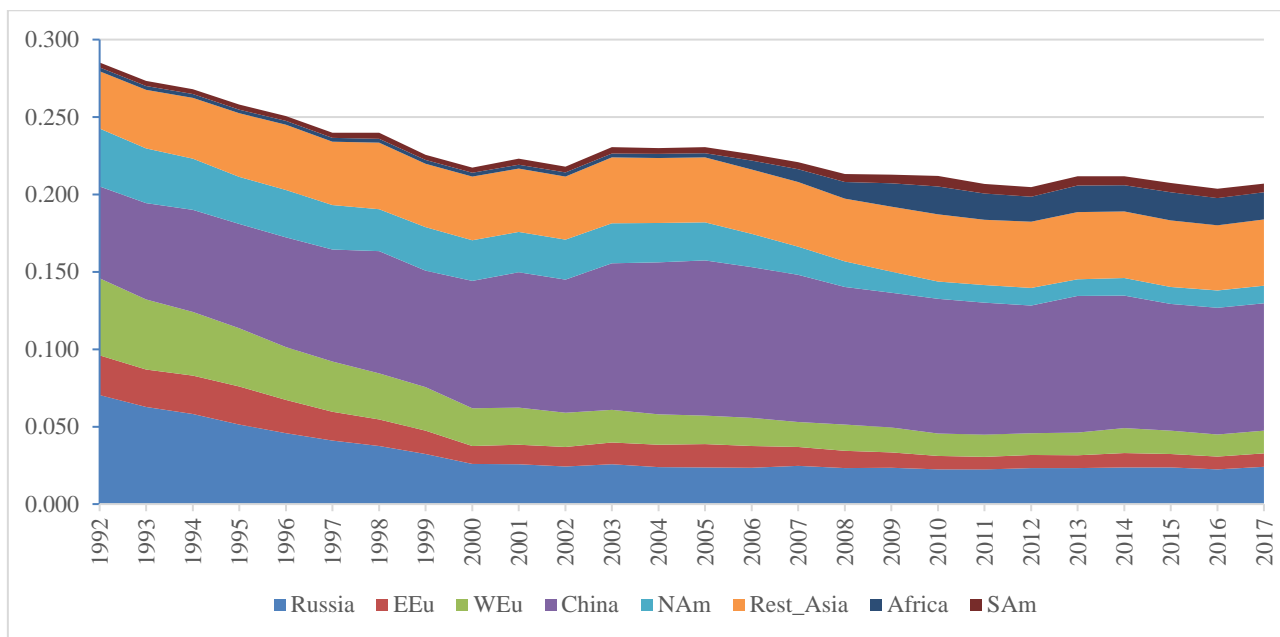
Figure 7: Model calculation of the source apportionment of the direct anthropogenic contribution to the annual average GEM
350 **concentrations at Villum. The DEHM model used two years (1990 and 1991) to spin up the model. Source regions: Russia = Russia;**
EEU = East Europe; WEu = West Europe; China = China; Africa = Africa; Sam = South America. Unit: ng m⁻³.
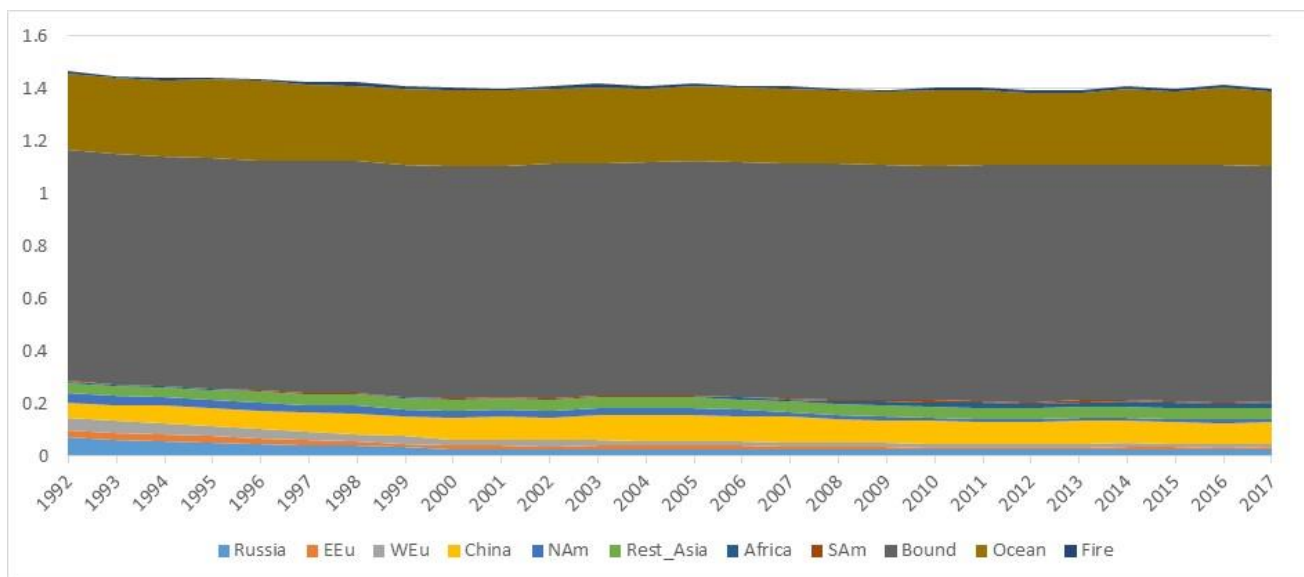
Figure 8: Model calculation of the source apportionment of annual average GEM at Villum. The DEHM model used two years (1990 and 1991) to spin up the model. In the model reemission from ocean and contribution from boundary conditions at equator included. Source regions: Russia = Russia; EEU = East Europe; WEu = West Europe; China = China; Africa = Africa; Sam = South America; Bound = Boundary Condition; Ocean = Ocean; Fire = Wildfire. Unit: ng m^{-3}.

Author Contribution

All co-authors were involved in the scientific discussions of the paper

Henrik Skov: Project leader and principal writer

Jens Hjorth: Co-writer, coordination of statistical analysis

Bjarne Jensen: Calibration, tests and setup of instruments

Christel Christoffersen: Calibration, tests and setup of instruments

Maria Bech Poulsen: Trend analysis and analysis of the relation between ozone and GEM

Jesper Baldtzer Liisberg: Analysis of depletion events

David Beddows: Trajectory clustering analysis and K-statistics.

Manual Dall'Osto: Trajectory clustering analysis and K-statistics as well as overall design of article

Jesper Heile Christensen: Model calculations by DEHM.

370 **Acknowledgement**

This study was founded by the Danish Environmental Protection Agency (DANCEA funds for Environmental Support to the Arctic Region) and by the European program ERA-PLANET project iGOSP and iCUBE. The Royal Danish Air Force is acknowledged for providing free transport of equipment to Station Nord, and the staff at Station Nord is especially acknowledged for excellent technical support. The Villum Foundation is gratefully acknowledged for financing the new
375 research station, Villum Research Station.

References

AMAP/UNEP. 2013. "Technical Background Report for the Global Mercury Assessment." In. Oslo, Norway and Geneva, Switzerland: Arctic Monitoring and Assessment Programme and UNEP. https://www.amap.no/documents/doc/Technical-Background-Report-for-the-Global-Mercury-Assessment-2013/848, 2013

380 Angot, H., A. Dastoor, F. De Simone, K. Gardfeldt, C. N. Gencarelli, I. M. Hedgecock, S. Langer, O. Magand, M. N. Mastromonaco, C. Nordstrom, K. A. Pfaffhuber, N. Pirrone, A. Ryjkov, N. E. Selin, H. Skov, S. J. Song, F. Sprovieri, A. Steffen, K. Toyota, O. Travnikov, X. Yang, and A. Dommergue. 'Chemical cycling and deposition of atmospheric mercury in Polar Regions: review of recent measurements and comparison with models', Atmospheric Chemistry and Physics, 16: 10735-63, 2016.

385 Ariya, P. A.; Skov, H.; Grage, M. L.; Goodsite, M. E., Gaseous Elemental Mercury in the Ambient Atmosphere: Review of the Application of Theoretical Calculations and Experimental Studies for Determination of Reaction Coefficients and Mechanisms with Halogens and Other Reactants. . Advances in Quantum Chemistry, 55, Chapter 4, 44-54, 2008.

Berg, T.; Pfaffhuber, K. A.; Cole, A. S.; Engelsen, O.; Steffen, A., Ten-year trends in atmospheric mercury concentrations, meteorological effects and climate variables at Zeppelin, Ny-Alesund. Atmos. Chem. Phys., 13 (13), 6575-6586, 2013.

390 Brandt, J., J. D. Silver, L. M. Frohn, C. Geels, A. Gross, A. B. Hansen, K. M. Hansen, G. B. Hedegaard, C. A. Skjoth, H. Villadsen, A. Zare, and J. H. Christensen. 'An integrated model study for Europe and North America using the Danish Eulerian Hemispheric Model with focus on intercontinental transport of air pollution', Atmospheric Environment, 53: 156-76, 2012.

Brooks, S.; Saiz-Lopez, A.; Skov, H.; Lindberg, S.; Plane, J. M. C.; Goodsite, M. E., The mass balance of mercury in the springtime polar environment. Geophys. Res. Lett., 33, L13812, 2006.

395 Chen, L., Y. X. Zhang, D. J. Jacob, A. L. Soerensen, J. A. Fisher, H. M. Horowitz, E. S. Corbitt, and X. J. Wang. 'A decline in Arctic Ocean mercury suggested by differences in decadal trends of atmospheric mercury between the Arctic and northern midlatitudes', Geophysical Research Letters, 42: 6076-83, 2015.

Christensen, J. H. 'The Danish Eulerian hemispheric model - A three-dimensional air pollution model used for the Arctic', Atmospheric Environment, 31: 4169-91, 1997.

400 Christensen, J. H., J. Brandt, L. M. Frohn, and H. Skov. 'Modelling of mercury in the Arctic with the Danish Eulerian Hemispheric Model', Atmospheric Chemistry and Physics, 4: 2251-57, 2004.

Cobbett, F. D.; Steffen, A.; Lawson, G.; Van Heyst, B. J., GEM fluxes and atmospheric mercury concentrations (GEM, RGM and Hg-P) in the Canadian Arctic at Alert, Nunavut, Canada (February-June 2005). Atmos. Environ. 41 (31), 6527-6543, 2007.

Cole, A. S.; Steffen, A.; Pfaffhuber, K. A.; Berg, T.; Pilote, M.; Poissant, L.; Tordon, R.; Hung, H., Ten-year trends of atmospheric mercury in the high Arctic compared to Canadian sub-Arctic and mid-latitude sites. Atmos. Chem. Phys. 13 (3), 1535-1545, 2013.

Dall'Osto, M.; Geels, C.; Beddows, D. C. S.; Boertmann, D.; Lange, R.; Nojgaard, J. K.; Harrison, R. M.; Simo, R.; Skov, H.; Massling, A., Regions of open water and melting sea ice drive new particle formation in North East Greenland. Sci Rep. 8, 10, 2018.

Dibble, T. S.; Zelie, M. J.; Mao, H., Thermodynamics of reactions of ClHg and BrHg radicals with atmospherically abundant free radicals. Atmos. Chem. Phys. 12 (21), 10271-10279, 2012.

Donohoue, D. L.; Bauer, D.; Cossairt, B.; Hynes, A. J., Temperature and pressure dependent rate coefficients for the reaction of Hg with Br and the reaction of Br with Br: A pulsed laser photolysis-pulsed laser induced fluorescence study. J. Phys. Chem. A, 110 (21), 6623-6632, 2006.

Durnford, D., A. Dastoor, D. Figueras-Nieto, and A. Ryjkov. 'Long range transport of mercury to the Arctic and across Canada', Atmospheric Chemistry and Physics, 10: 6063-86, 2010..

Fisher, J. A.; Jacob, D. J.; Soerensen, A. L.; Amos, H. M.; Steffen, A.; Sunderland, E. M., Riverine source of Arctic Ocean mercury inferred from atmospheric observations. Nat. Geosci. 5 (7), 499-504, 2012.

Freud, E., R. Krejci, P. Tunved, R. Leaitch, Q. T. Nguyen, A. Massling, H. Skov, and L. Barrie. 'Pan-Arctic aerosol number size distributions: seasonality and transport patterns', Atmospheric Chemistry and Physics, 17: 8101-28. 2017.

Frohn, L. M., J. H. Christensen, and J. Brandt. 'Development of a high-resolution nested air pollution model - The numerical approach', Journal of Computational Physics, 179: 68-94, 2002.

Goodsite, M. E., J. M. C. Plane, and H. Skov. 'A theoretical study of the oxidation of Hg-0 to HgBr$_2$ in the troposphere', Environmental Science & Technology, 38: 1772-76, 2004.

Goodsite, M., J. Plane, and H. Skov. 'A Theoretical Study of the Oxidation of Hg0 to HgBr$_2$ in the Troposphere (vol 38, pg 1772, 2004)', Environmental Science & Technology, 46: 5262-62, 2012b.

Heidam, N. Z., J. Christensen, P. Wahlin, and H. Skov. 'Arctic atmospheric contaminants in NE Greenland: levels, variations, origins, transport, transformations and trends 1990-2001', Science of the Total Environment, 331: 5-28, 2004.

Heidam, N. Z., P. Wahlin, and J. H. Christensen. 'Tropospheric gases and aerosols in northeast Greenland', Journal of the Atmospheric Sciences, 56: 261-78, 1999.

Hirdman, D., J. F. Burkhart, H. Sodemann, S. Eckhardt, A. Jefferson, P. K. Quinn, S. Sharma, J. Strom, and A. Stohl. 'Long-term trends of black carbon and sulphate aerosol in the Arctic: changes in atmospheric transport and source region emissions', Atmospheric Chemistry and Physics, 10: 9351-68, 2010.

Holmes, C. D., D. J. Jacob, E. S. Corbitt, J. Mao, X. Yang, R. Talbot, and F. Slemr. 'Global atmospheric model for mercury including oxidation by bromine atoms', Atmospheric Chemistry and Physics, 10: 12037-57, 2010.

Jiskra, M., J. E. Sonke, D. Obrist, J. Bieser, R. Ebinghaus, C. L. Myhre, K. A. Pfaffhuber, I. Wangberg, K. Kyllonen, D. Worthy, L. G. Martin, C. Labuschagne, T. Mkololo, M. Ramonet, O. Magand, and A. Dommergue. 'A vegetation control on seasonal variations in global atmospheric mercury concentrations', Nature Geoscience, 11: 244-251, 2018.

Kamp, J., H. Skov, B. Jensen, and L. L. Sorensen. 'Fluxes of gaseous elemental mercury (GEM) in the High Arctic during atmospheric mercury depletion events (AMDEs)', Atmospheric Chemistry and Physics, 18: 6923-38, 2018.

Lamborg, C. H., C. R. Hammerschmidt, K. L. Bowman, G. J. Swarr, K. M. Munson, D. C. Ohnemus, P. J. Lam, L. E. Heimburger, M. J. A. Rijkenberg, and M. A. Saito. 'A global ocean inventory of anthropogenic mercury based on water column measurements', Nature, 512: 65-69, 2014.

Moller, A. K.; Barkay, T.; Abu Al-Soud, W.; Sorensen, S. J.; Skov, H.; Kroer, N., Diversity and characterization of mercury-resistant bacteria in snow, freshwater and sea-ice brine from the High Arctic. FEMS Microbiol. Ecol. 75 (3), 390-401, 2011.

Muntean, M., G. Janssens-Maenhout, S. J. Song, A. Giang, N. E. Selin, H. Zhong, Y. Zhao, J. G. J. Olivier, D. Guizzardi, M. Crippa, E. Schaaf, and F. Dentener. 'Evaluating EDGARv4.tox2 speciated mercury emissions ex-post scenarios and their impacts on modelled global and regional wet deposition patterns', Atmospheric Environment, 184: 56-68, 2018.

Muntean, M., G. Janssens-Maenhout, S. Song, N. E. Selin, J. G. J. Olivier, D. Guizzardi, R. Maas, and F. Dentener. 'Trend analysis from 1970 to 2008 and model evaluation of EDGARv4 global gridded anthropogenic mercury emissions', Science of the Total Environment, 494-495: 337-50, 2014.

Nguyen, Q. T., H. Skov, L. L. Sorensen, B. J. Jensen, A. G. Grube, A. Massling, M. Glasius, and J. K. Nojgaard. 'Source apportionment of particles at Station Nord, North East Greenland during 2008-2010 using COPREM and PMF analysis', Atmospheric Chemistry and Physics, 13: 35-49, 2013.

NOAA: http://www.cpc.ncep.noaa.gov/data/teledoc/nao.shtml, 2018a

NOAA: http://www.cpc.ncep.noaa.gov/products/precip/CWlink/daily_ao_index/ao.shtml, 2018b.

Obrist, D.; Kirk, J. L.; Zhang, L.; Sunderland, E. M.; Jiskra, M.; Selin, N. E., A review of global environmental mercury processes in response to human and natural perturbations: Changes of emissions, climate, and land use. Ambio. 47 (2), 116-140, 2018.

Outridge, P. M.; Macdonald, R. W.; Wang, F.; Stern, G. A.; Dastoor, A. P., A mass balance inventory of mercury in the Arctic Ocean. Environmental Chemistry 5, 1-23, 2008.

Pacyna, E. G., J. M. Pacyna, K. Sundseth, J. Munthe, K. Kindbom, S. Wilson, F. Steenhuisen, and P. Maxson. 'Global emission of mercury to the atmosphere from anthropogenic sources in 2005 and projections to 2020', Atmospheric Environment, 44: 2487-99, 2010.

Pirrone, N., S. Cinnirella, X. Feng, R. B. Finkelman, H. R. Friedli, J. Leaner, R. Mason, A. B. Mukherjee, G. B. Stracher, D. G. Streets, and K. Telmer. 'Global mercury emissions to the atmosphere from anthropogenic and natural sources', Atmospheric Chemistry and Physics, 10: 5951-64, 2010.

Schroeder, W. H., K. G. Anlauf, L. A. Barrie, J. Y. Lu, A. Steffen, D. R. Schneeberger, and T. Berg. 'Arctic springtime depletion of mercury', Nature, 394: 331-32, 1998.

470 Skamarock, W. C., J. B., Dudhia, J., Gill, D. O., Barker, D. M., Duda, M. G., Huang, X.-Y., Wang, W., and Powers, J. G. A description of the Advanced Research WRF version 3, p 113, 2008.

Skov, H., S. B. Brooks, M. E. Goodsite, S. E. Lindberg, T. P. Meyers, M. S. Landis, M. R. B. Larsen, B. Jensen, G. McConville, and J. Christensen. 'Fluxes of reactive gaseous mercury measured with a newly developed method using relaxed eddy accumulation', Atmospheric Environment, 40: 5452-63, 2006.

475 Skov, H., J. H. Christensen, M. E. Goodsite, N. Z. Heidam, B. Jensen, P. Wahlin, and G. Geernaert. 'Fate of elemental mercury in the arctic during atmospheric mercury depletion episodes and the load of atmospheric mercury to the arctic', Environmental Science & Technology, 38: 2373-82, 2004.

Soerensen, A. L., D. J. Jacob, D. G. Streets, M. L. I. Witt, R. Ebinghaus, R. P. Mason, M. Andersson, and E. M. Sunderland. 'Multi-decadal decline of mercury in the North Atlantic atmosphere explained by changing subsurface seawater
480 concentrations', Geophysical Research Letters, 39, 2012.

Soerensen, A. L., E. M. Sunderland, C. D. Holmes, D. J. Jacob, R. M. Yantosca, H. Skov, J. H. Christensen, S. A. Strode, and R. P. Mason. 'An Improved Global Model for Air-Sea Exchange of Mercury: High Concentrations over the North Atlantic', Environmental Science & Technology, 44: 8574-80, 2010.

Steen, A. O.; Berg, T.; Dastoor, A. P.; Durnford, D. A.; Hole, L. R.; Pfaffhuber, K. A., Dynamic exchange of gaseous elemental
485 mercury during polar night and day. Atmos. Environ. 43 (35), 5604-5610, 2009.

Steffen, A., T. Douglas, M. Amyot, P. Ariya, K. Aspmo, T. Berg, J. Bottenheim, S. Brooks, F. Cobbett, A. Dastoor, A. Dommergue, R. Ebinghaus, C. Ferrari, K. Gardfeldt, M. E. Goodsite, D. Lean, A. J. Poulain, C. Scherz, H. Skov, J. Sommar, and C. Temme. 'A synthesis of atmospheric mercury depletion event chemistry in the atmosphere and snow', Atmospheric Chemistry and Physics, 8: 1445-82, 2008.

490 Steffen, A.; Lehnherr, I.; Cole, A.; Ariya, P.; Dastoor, A.; Durnford, D.; Kirk, J.; Pilote, M., Atmospheric mercury in the Canadian Arctic. Part I: A review of recent field measurements. Sci. Total Environ. 509, 3-15, 2015.

UNEP. 2013. "Global Mercury Assessment: Sources, Emissions, Releases and Environmental Transport." In. Geneva, Switzerlsand: UNEP Chemicals Branch, 2013.

UNEP.   Minamata   Convention   on   Mercury.   UNEP.   October   2013.
495 http://www.mercuryconvention.org/Convention/tabid/3426/Default.aspx, 2013b.

van der Werf, G. R., J. T. Randerson, L. Giglio, G. J. Collatz, P. S. Kasibhatla, and A. F. Arellano. 'Interannual variability in global biomass burning emissions from 1997 to 2004', Atmospheric Chemistry and Physics, 6: 3423-41, 2006.

Wang, S. Y.; McNamara, S. M.; Moore, C. W.; Obrist, D.; Steffen, A.; Shepson, P. B.; Staebler, R. M.; Raso, A. R. W.; Pratt, K. A., Direct detection of atmospheric atomic bromine leading to mercury and ozone depletion. Proc. Natl. Acad. Sci. U. S.
500 A. 116 (29), 14479-14484, 2019.